Modern Physics Letters B
Vol. 28, No. 6 (2014) 1450043 (8 pages)
© World Scientific Publishing Company
DOI: 10.1142/S0217984914500432

World Scientific
www.worldscientific.com

Effects of ZnO layer on anisotropy magnetoresistance of $Ni_{81}Fe_{19}$ films

Shuyun Wang*, Yuanmei Gao, Tiejun Gao, Yuan He, Hui Zhang and Yuan Yao

College of Physics and Electronics,
Shandong Normal University, Ji'nan 250014, China
**wangshuyun65@163.com*

Received 1 October 2013
Revised 12 January 2014
Accepted 20 January 2014
Published 25 February 2014

A series of Ta (4 nm)/ZnO (t nm)/$Ni_{81}Fe_{19}$ (20 nm)/ZnO (t nm)/Ta (3 nm) magnetic thin films were prepared on lower experimental conditions by magnetron sputtering method. Effects of ZnO layer thickness and substrate temperature on anisotropic magnetoresistance and magnetic properties of these $Ni_{81}Fe_{19}$ films have been investigated. The experiment results show that the anisotropic magnetoresistance value of the $Ni_{81}Fe_{19}$ film is enhanced with the increasing of the inserted ZnO layer thickness. When the ZnO thickness is 2 nm, the anisotropic magnetoresistance value achieves the maximum. In addition, the anisotropic magnetoresistance of the $Ni_{81}Fe_{19}$ film is also enhanced with the increasing of substrate temperature, and when the temperature is 450°C, the anisotropic magnetoresistance reaches the maximum. The anisotropic magnetoresistance value of 20 nm $Ni_{81}Fe_{19}$ films with 2 nm ZnO layer can achieve 3.63% at 450°C which is enhanced 11.6% compare with the films without ZnO layer.

Keywords: Permalloy thin film; anisotropic magnetoresistance; ZnO layer; substrate temperature.

1. Introduction

At present, although the anisotropic magnetoresistance (AMR) heads are progressively replaced by spin-valve and tunnel junction heads in magnetic disk drives, the research and development of NiFe films for the magnetic sensor application are still widely followed[1–7] because of the advantages such as low cost, simple structure, high sensitivity and lower saturation field, especially angle sensitivity which seems the irreplaceable outstanding advantage. The novel magnetic sensor based on NiFe films will be applied broadly in the geomagnetic navigation, automotive compass, and the posture positioning system of the unmanned aerial vehicle (UAV). With the growing demand for the AMR NiFe magnetic sensor, it has become necessary to fabricate NiFe films which have higher AMR value, higher sensitivity, lower

www.spm.com.cn

coercive force and thinner thickness under the optimum conditions. However, relevant research indicates that the crystal quality of NiFe films will decline significantly if the thickness of NiFe films is reduced, while the shunting effect of the buffer layer and protective layer is enhancing[8–11] with reducing the thickness of NiFe films. Besides, the microstructure of NiFe films is damaged by magnetic dead layer which is generated by solid-phase reaction between the adjacent layers. These factors will lead that the AMR of NiFe films decreases significantly. In order to solve these problems, Wang *et al.*,[12] Lei *et al.*,[13] Chongjun *et al.*,[14] and Minghua *et al.*[15] investigated the effects of nano oxide layer (NOL) on the performance of NiFe films by inserting $A1_2O_3$ and MgO material between NiFe and metal buffer layer, and between NiFe and metal protective layer. The experimental results show that by inserting an oxide layer we can reduce the shunting effects of the buffer layer and protective layer, restrain the generation of magnetic dead layer and enhance the mirror effect, which can reflect the conduction electrons, thereby effectively improving the AMR of NiFe films. Hence, finding the right oxidation inserted layer is a way to improve the AMR. The crystallization temperature of ZnO is lower than that of $A1_2O_3$ and MgO, which is beneficial to inhibit diffusion of the solid phase. If ZnO is used as a new oxide inserted layer, it will get a better crystallinity at the same low temperature, enhance the mirror effect which can reflect the conduction electron and improve the AMR and sensitivity of NiFe films. In this paper, we study the effect of inserted ZnO layer on AMR of NiFe film. In addition, we have adopted lower experimental conditions such as the base pressure is 5.8×10^{-4} Pa and the working gas pressure is 0.5 Pa. But in many other studies the base pressure was less than 10^{-5} Pa and the working gas pressure was below 0.5 Pa. $Ni_{81}Fe_{19}$ film grew at different substrate temperature instead of the annealing treatment in other studies.[10–13] A better result was obtained.

2. Experiment

The Ta (4 nm)/ZnO (t nm)/$Ni_{81}Fe_{19}$ (20 nm)/ZnO (t nm)/Ta (3 nm) films are sputtered on the corning glass substrates with a magnetron sputtering system (JGP-450) at various substrate temperature: 20, 250, 300, 350, 400, 450, and 500°C, respectively. The Ta and NiFe layers were deposited from Ta and $Ni_{81}Fe_{19}$ alloy targets by dc sputtering, while the ZnO layer was deposited from ZnO ceramic target by rf sputtering. The film thickness in the artificial structure, referring to the physical thickness, was estimated based on the deposition rate which can be calculated using the total deposited film thickness plotted against deposition time. Film thickness was measured by weighting method and averaged for three measurements. First, the weight m_1 of the Corning glass of 4 cm^2 was measured. Then the coating material was sputtered on the Corning glass for time τ. The weight m_2 of the 4 cm^2 Corning glass with sputtered coating material was measured again, and then the sputtering deposition rate was calculated by the following formulas. $v = t/\tau$, $t = (m_2 - m_1)/s\rho$. In the formulas, v is the sputtering deposition rate, t

www.spm.com.cn

is the film thickness, τ is the sputtering time, s is the surface area of the glass, and the ρ is the density of the sputtered material. In this way, the sputtering deposition rates are about 0.258 nm/s (Ta), 0.273 nm/s ($Ni_{81}Fe_{19}$) and 0.133 nm/s (ZnO). Correspondingly, the Ta films with thickness of 4 nm were deposited for 16 s, and the NiFe films with thickness of 20 nm were deposited for 73 s. The ZnO films with thickness of 0.5–4 nm were deposited for 4–30 s. The base pressure is 5.8×10^{-4} Pa and the working gas pressure of 99.99% Ar is 0.5 Pa. During the sputtering process, about 14 kA/m magnetic field was supplied by a set of permanent magnet along the substrate surface to induce uniaxial anisotropy in the films. AMR value of permalloy films was measured by noncollinear four-point probe method (BKT-1). In order to reduce the error caused by the ohmic contact electrode, we adopted noncollinear four point probe method for measuring AMR. The probes are nonmagnetic gold-plated elastic probe. The distribution of the four probes is a square of about 5 mm on a side. The microstructure and crystal orientation of permalloy films were analyzed by XRD(TD-3000) with Cu Ka radiation. The surface topography of $Ni_{81}Fe_{19}$ films were measured by AFM(BY-3000).

3. Results and Discussion

3.1. *Effect of the ZnO layer thickness on anisotropic magnetoresistance of permalloy films*

A set of the films Ta (4 nm)/ZnO (t nm)/$Ni_{81}Fe_{19}$ (20 nm)/ZnO (t nm)/Ta (3 nm) are prepared at 450°C, with $t = 0$, 0.5, 1, 1.5, 2, 3 and 4 nm, respectively. Figure 1(a) is the AMR curves and Fig. 1(b) is the AMR value curve of films Ta (4 nm)/ZnO (t nm)/$Ni_{81}Fe_{19}$ (20 nm)/ZnO (t nm)/Ta (3 nm). As shown in Fig. 1(b), the AMR value first declines from 3.0% to 2.73% when $t = 0$ to 0.5 nm, then increases quickly with t increasing, and the AMR reaches maximum 3.63% when $t = 2$, and then tends to be stable.

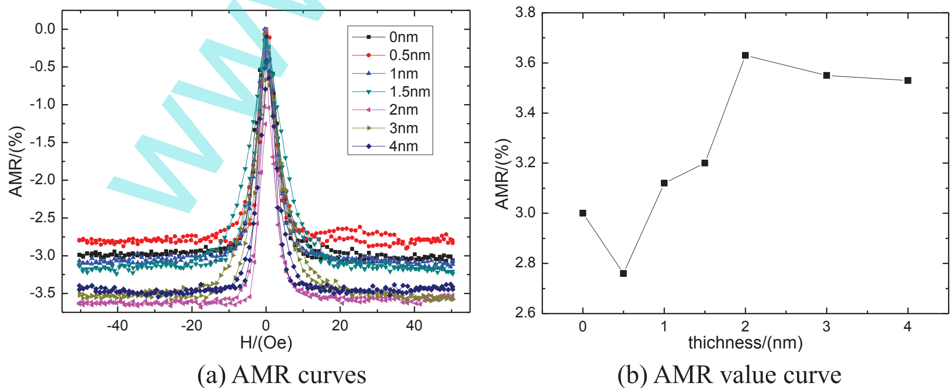

Fig. 1. (Color online) AMR curves of the films Ta (4 nm)/ZnO (t nm)/$Ni_{81}Fe_{19}$ (20 nm)/ZnO (t nm)/Ta (3 nm).

www.spm.com.cn

The above results can be analyzed as follows. When $t = 0.5$ nm, due to reduced ZnO sputtering onto the Ta film, it leads to the formation of discrete structure of ZnO island. The normal growth of $Ni_{81}Fe_{19}$ layer is strongly influenced by this island structure, thereby the AMR decreasing. With the increasing of the ZnO layer thickness, the continuous ZnO layer between Ta layer and $Ni_{81}Fe_{19}$ layer is formed. The continuous ZnO layer significantly suppress the interface reactions and the inter-diffusions of Fe, Ni and Ta atom between the Ta layer and the NiFe layer, and decrease the current shunting of the Ta layers, leading to the further enhancement of the AMR. In addition, according to the electronic reflection effect, the ZnO layers play an important role in specular reflection.[16] Due to the significantly enhanced specular reflection of conduction electrons while conserving the spin direction occurring at the ZnO/NiFe and NiFe/ZnO interfaces, the mean free path of the spin electrons was extended and thus the resistivity of the NiFe films was significantly decreased, leading to a high AMR value.[12–15] As t further increases above 2 nm, the effect of the "mirror reflection" layer to conduction electron scattering no longer increase with the ZnO layer thickness increasing, thus, the AMR value tends to be stable.

3.2. *Influence of substrate temperature on AMR of $Ni_{81}Fe_{19}$ films with ZnO layer*

A series of films Ta (4 nm)/ZnO (2 nm)/$Ni_{81}Fe_{19}$ (20 nm)/ZnO (2 nm)/Ta (3 nm) and Ta (4 nm)/$Ni_{81}Fe_{19}$ (20 nm)/Ta (3 nm) are prepared with the various substrate temperature: 20, 250, 300, 350, 400, 450 and 500°C, respectively. Figure 2(a) is the AMR curves of these films dependence on the substrate temperature. Figure 2(b) is the AMR value curves. In Fig. 2(b), it is clear that the AMR value increases at first and then decreases with the substrate temperature increasing. The AMR value of the films with ZnO layer arrive the maximum 3.63% at 450°C. For comparison,

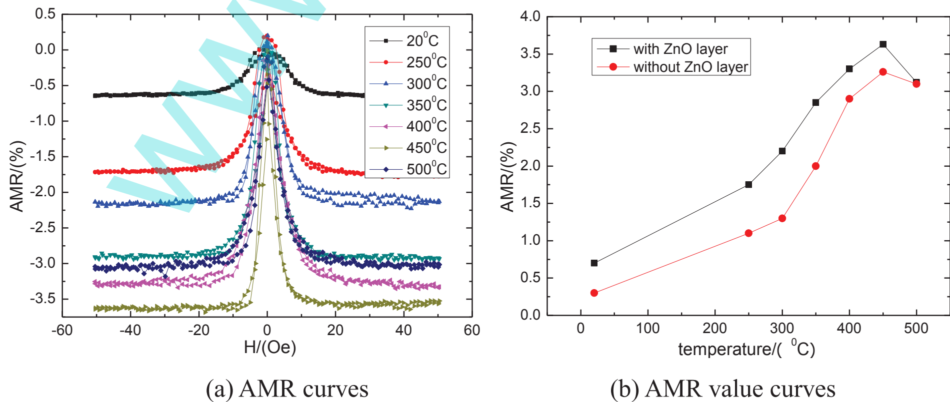

(a) AMR curves (b) AMR value curves

Fig. 2. (Color online) AMR value of $Ni_{81}Fe_{19}$ films dependence on the substrate temperature.

www.spm.com.cn

Ta (4 nm)/$Ni_{81}Fe_{19}$ (20 nm)/Ta (3 nm) films are prepared in the same conditions and the maximum AMR value is 3.25%, which is lower than the films with ZnO layer by about 11.6%. It shows that ZnO layer has a significant role to improve the AMR value of permalloy film.

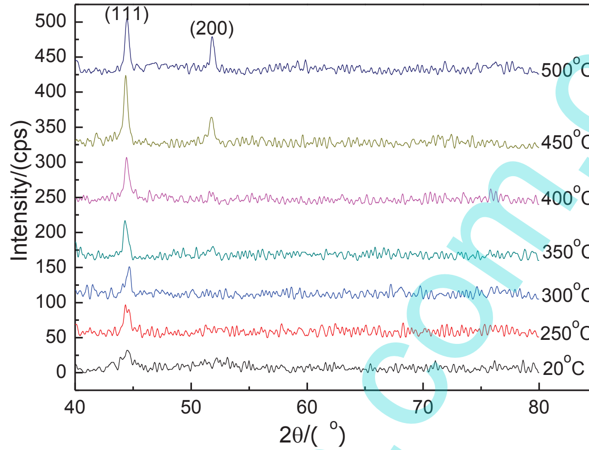

Fig. 3. (Color online) XRD patterns of the films Ta (4 nm)/ZnO (2 nm)/$Ni_{81}Fe_{19}$ (20 nm)/ZnO (2 nm)/Ta (3 nm) prepared at different temperatures.

To explain the above results, X-ray diffraction (XRD) was used to research the influence of substrate temperature on structure of the films Ta (4 nm)/ZnO (2 nm)/$Ni_{81}Fe_{19}$ (20 nm)/ZnO (2 nm)/Ta (3 nm). Figure 3 is the XRD patterns of the 20 nm $Ni_{81}Fe_{19}$ films with 2 nm ZnO layer. All the diffraction angles 2θ of diffraction peak are about 44.4° and 51.8°, corresponding to the indices of crystallographic plane (111) and (200) of $Ni_{81}Fe_{19}$, respectively. The substrate temperature has significant influences on the microstructure of permalloy films. In Fig. 3, with the substrate temperature rising, the film (111) diffraction peak increased first and then decreased. When the substrate temperature is 450°C, the (111) diffraction peak intensity reaches the strongest. By the Scherrer formula, the grain size of the films is calculated, and the result is 8.35, 12.21, 13.41, 16.27, 18.93 and 16.78 nm when the substrate temperature is 250, 300, 350, 400, 450 and 500°C, respectively. The corresponding peak half width is 1.02°, 0.695°, 0.632°, 0.521°, 0.448° and 0.505°, respectively. It is obvious that when the substrate temperature is 450°C the films have the biggest grain size and the best degree of crystallinity alone the (111) crystallization direction, corresponding to the highest AMR value. In addition, with the substrate temperature rise higher, the energy of deposited atoms will be gradually increasing and the ability of its transverse diffusion will be strengthen. It effectively reduced the stress distribution between the membrane in inter-granular and substrate, and makes the thin film defects decrease. Thus, the microstructure of films dramatically changes as well. The above two reasons cause a

www.spm.com.cn

decline in the grain boundary. According to the scattering mechanism, the reducing crystal boundary causes the weak electronic scattering, further lead to the increase on AMR value.[12–15] When the substrate temperature is greater than or equal to 450°C, it appears (200) diffraction peak where the 2θ is 51.8°, which reduce the unipolarity of (111) preferred orientation. But this preferred orientation is just the easy magnetization axis of permalloy films. Thereby it influences the anisotropy of permalloy films and leads to decrease of AMR at 500°C. The above analysis is consistent with the curves in Fig. 2. When the substrate temperature is 450°C, the AMR value achieves to the maximum 3.63%, and then decreases with the temperature rising. Besides, the higher substrate temperature leads to the diffusion of atoms between adjacent layers. It reduced the actual thickness of permalloy film, which influence the diffraction intensity and AMR value of permalloy films.

The surface topography of Ta (4 nm)/ZnO (2 nm)/$Ni_{81}Fe_{19}$ (20 nm)/ZnO (2 nm)/Ta (3 nm) prepared at different substrate temperature is further measured by AFM, shown in Fig. 4. Table 1 shows the roughness and particle sizes of Ta/ZnO/$Ni_{81}Fe_{19}$/ZnO/Ta films prepared at different substrate temperature. It

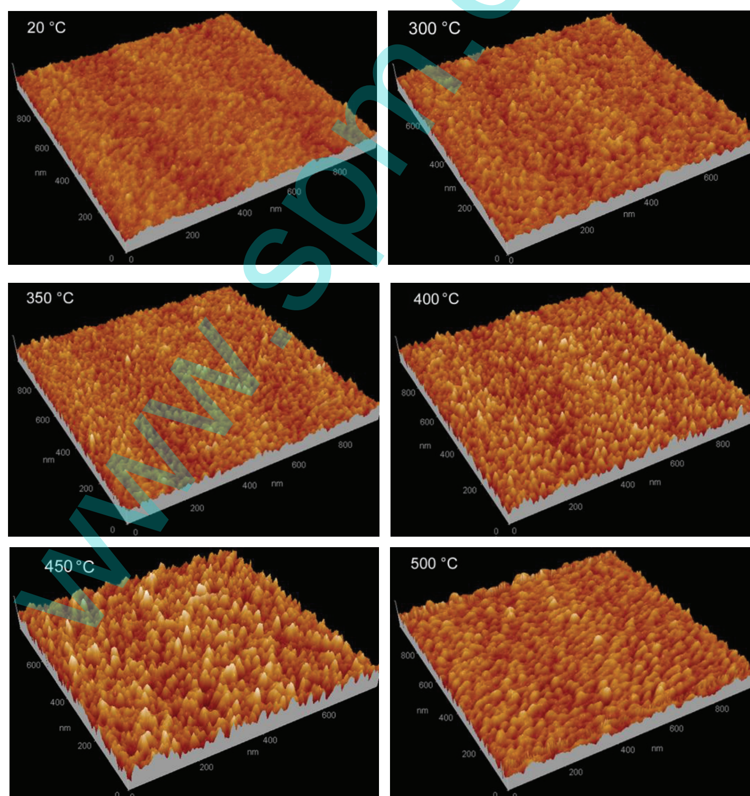

Fig. 4. (Color online) AFM images about surface morphology of Ta (4 nm)/ZnO (2 nm)/$Ni_{81}Fe_{19}$ (20 nm)/ZnO (2 nm)/Ta (3 nm) films prepared at different substrate temperature.

www.spm.com.cn

Table 1. Roughness and particle sizes of Ta (4 nm)/ZnO (2 nm)/$Ni_{81}Fe_{19}$ (20 nm)/ZnO (2 nm)/Ta (3 nm) films prepared at different substrate temperature.

Substrate temperature (°C)	20	300	350	400	450	500
Root mean square (nm)	1.50	1.84	1.88	1.93	2.25	2.04
Particle sizes (nm)	13.50	16.2	19.71	20.21	22.12	22.42

is clear to see from Fig. 4 and Table 1 that significant change takes place at the surface morphology of films with the substrate temperature rising. At a lower temperature, the surface morphology of the deposited film more appeared as a kind of amorphous state. With the temperature rising, the particles of the NiFe film are more obvious, and the particle size becomes bigger. When the substrate temperature is 450°C the roughness of the film reaches to the maximum. This is because the unipolarity of (111) preferred orientation of NiFe films crystallization reached the strongest at 450°C. Due to the anisotropy of crystal growth, the average particle size of thin film surface is not the biggest. With the (220) crystal orientation of NiFe films appear and enhanced in 500°C, the particle of film deposited at 500°C appears more rounded and the average particle size of thin film surface is bigger than that of film deposited at 450°C.

4. Conclusion

Inserting ZnO layer between $Ni_{81}Fe_{19}$ film and buffer layer, and between $Ni_{81}Fe_{19}$ film and protective layer is a way to improve the AMR of $Ni_{81}Fe_{19}$ film. The experiment results show that the AMR value of the $Ni_{81}Fe_{19}$ film is enhanced with the increasing of the inserted ZnO layer thickness. When the ZnO thickness is 2 nm, the AMR value reaches the maximum, and then tends to be stable. In addition, increasing substrate temperature can also enhance the AMR value of the $Ni_{81}Fe_{19}$ film, and when the temperature is 450°C, the AMR value reaches the maximum. The AMR value of 20 nm $Ni_{81}Fe_{19}$ films with 2 nm inserted ZnO layer can reaches 3.63% at 450°C. Comparing with the films without ZnO layer it is increased by 11.6%.

Acknowledgments

This study was supported by the Shandong Provincial Natural Science Foundation, China (Grant No. ZR2013EMM009) and the National Natural Science Foundation of China (Grant No. 11304187).

References

1. H. Hauser *et al.*, *Sens. Actuators A* **106** (2003) 121–125.
2. L. Ding *et al.*, *Appl. Phys. Lett.* **96** (2010) 052515.
3. S. Y. Wang, T. J. Gao,C. T. Wang and J. F. He, *J. Alloys Compds.* **554** (2013) 405–407.

www.spm.com.cn

4. S. Y. Wang, C. T. Wang, Y. M. Gao, T. J. Gao and J. F. He,*J. Alloys Compds.* **575** (2013) 419–422.
5. P. Wu *et al.*, *Rare Metals* **26**(2) (2007) 176–181.
6. J. Choi *et al.*, *Thin Solid Films* **519** (2011) 8394–8396.
7. J. Singh *et al.*, *J. Magn. Magn. Mater.* **324** (2012) 999–1005.
8. C. Jin *et al.*, *Chin. J. Vac. Sci. Technol.* **S1**(28) (2008) 5–8.
9. G. H. Yu *et al.*, *Chin. J. Vac. Sci. Technol.* **21**(5) (2001) 419–422.
10. G. H. Yu *et al.*, *Appl. Phys. Lett.* **80**(3) (2002) 455.
11. T. Miyazaki, T. Ajima and F. Sato, *J. Magn. Magn. Mater.* **81** (1989) 86–90.
12. D. W. Wang *et al.*, *Vac. Electron.* **3** (2007) 63–68.
13. L. Ding *et al.*, *Appl. Phys. Lett.* **94** (2009) 162506.
14. C. J. Zhao *et al.*, *Appl. Phys. Lett.* **101** (2012) 072404.
15. M. H. Li *et al.*, *J. Magn. Magn. Mater.* **324**(1) (2012) 1–3.
16. B. Dieny, M. Li, S. H. Liao, C. Horng and K. Ju, *J. Appl. Phys.* **88**(7) (2000) 4140.

www.spm.com.cn